DETERMINATION OF THE BEST METHODOLOGY FOR BATHYMETRY MAPPING USING SPOT 6 IMAGERY: A STUDY OF 12 EMPIRICAL ALGORITHMS

Masita Dwi Mandini Manessa[1*], Muhammad Haidar[2], Maryani Hastuti[3], Diah Kirana Kresnawati[1]
[1]Geodesy Department, Pakuan University, Bogor, Indonesia
[2]Thematic Mapping Division, Geospatial Information Agency of Indonesia, Bogor, Indonesia
[2]Remote Sensing Application Center, Indonesian National Institute of Aeronautics and Space, Jakarta, Indonesia
*e-mail: m.manessa@outlook.com

Received: 8 November 2017; Revised: 22 December 2017; Approved: 22 December 2017

Abstract. For the past four decades, many researchers have published a novel empirical methodology for bathymetry extraction using remote sensing data. However, a comparative analysis of each method has not yet been done. Which is important to determine the best method that gives a good accuracy prediction. This study focuses on empirical bathymetry extraction methodology for multispectral data with three visible band, specifically SPOT 6 Image. Twelve algorithms have been chosen intentionally, namely, 1) Ratio transform (RT); 2) Multiple linear regression (MLR); 3) Multiple nonlinear regression (RF); 4) Second-order polynomial of ratio transform (SPR); 5) Principle component (PC); 6) Multiple linear regression using relaxing uniformity assumption on water and atmosphere (KNW); 7) Semiparametric regression using depth-independent variables (SMP); 8) Semiparametric regression using spatial coordinates (STR); 9) Semiparametric regression using depth-independent variables and spatial coordinates (TNP), 10) bagging fitting ensemble (BAG); 11) least squares boosting fitting ensemble (LSB); and 12) support vector regression (SVR). This study assesses the performance of 12 empirical models for bathymetry calculations in two different areas: Gili Mantra Islands, West Nusa Tenggara and Menjangan Island, Bali. The estimated depth from each method was compared with echosounder data; RF, STR, and TNP results demonstrate higher accuracy ranges from 0.02 to 0.63 m more than other nine methods. The TNP algorithm, producing the most accurate results (Gili Mantra Island RMSE = 1.01 m and R^2=0.82, Menjangan Island RMSE = 1.09 m and R^2=0.45), proved to be the preferred algorithm for bathymetry mapping.

Keywords: *bathymetry; SPOT 6; empirical methodology; multispectral image*

1 INTRODUCTION

Bathymetry data is important for ship traffic, conservation, coastal zoning and other environmental issues. Traditional bathymetric charts are collected using a single multibeam echo-sounders of ship-borne surveying. This method gives a satisfactory accuracy in water depths of up to 200 m. Instead, these methods are limited by their high costs, areal coverage, and time consumption. This limitation became an important issue especially for a nation that has a long coastal area, such as Canada, Indonesia, Russia, and Philippine.

Remote sensing has been suggested as an alternative tool for mapping the bathymetry especially for shallow water environment (Lyzenga 1978; Kanno *et al.*

2011). In this study, satellite derives bathymetry (here and after as SDB) term was used to define the remote sensing method for bathymetry extraction. The SDB technique for multispectral image start appear in 1970 proposed by Polycin *et al.* (1970), a prototype model based on a ratio of reflected radiation in at least two spectral bands in the visible region of the spectrum, was used to determine water depth. A decade after, for the first time used a commercial satellite data LANDSAT TM to extract the depth of using a linearized regression of single band (Lyzenga 1985), this method was based on previous publication (Lyzenga 1978). Since that time the algorithm has been re-developed and applied to the newest multispectral image: LANDSAT-TM and ETM (Clark *et al.* 1987; Van Hengel and Spltzer 1991; Bierwirth *et al.* 1993; Daniell 2008), SPOT 4 and SPOT 5 (Melsheimer and Chin 2001; Lafon *et al.* 2002; Liu *et al.* 2010; Sánchez-Carnero *et al.* 2014), IKONOS (Stumpf *et al.* 2003; Hogrefe *et al.* 2008; Su *et al.* 2014), QuickBird (Conger *et al.* 2006; Mishra *et al.* 2006; Lyons *et al.* 2011), LANDSAT-OLI (Pacheco *et al.* 2015; Vinayaraj *et al.* 2016; Kabiri 2017; Pushparaj and Hegde 2017), and Worldview-2 (Lee and Kim 2011; Deidda and Sanna 2012; Doxani *et al.* 2012; Bramante *et al.* 2013; Kanno *et al.* 2013; Yuzugullu and Aksoy 2014; Eugenio *et al.* 2015; Manessa *et al.* 2016b; Guzinski *et al.* 2016; Hernandez and Armstrong 2016; Kibele and Shears 2016; Manessa *et al.* 2016a).

Overall, SDB empirical algorithm can be divided into two types, first, the empirical algorithm that based on pixel radiance/reflectance value and second the combination of pixel radiance/reflectance value and the spatial information. This study focus on an empirical algorithm that based on pixel radiance/reflectance value and the set up was inspired by previous studies (Arya *et al.* 2016; Mohamed *et al.* 2017). But even so, both studies compared less number of an empirical algorithm. Early investigators analyzing SPOT 6/7 data for its utility in assessing bathymetry assessed the four extensions of Lyzenga's SDB algorithm for turbid water (Arya *et al.* 2016) and a new statistical approach (Mohamed *et al.* 2017), those studies have concluded that SPOT 6/7 performed accurately in the bathymetry mapping.

Afterwards, no published work exists on comparing all published empirical SDB algorithm on the use of SPOT 6 data for bathymetry mapping. Our research focuses on the finding the best empirical SDB algorithm for SPOT 6 multispectral data. Twelve empirical SDB algorithm was intensionally chosen: 1) Ratio transform (henceforth named "RT") by Stumpt *et al.* (2003); 2) Multiple linear regression (henceforth named "MLR") by Lyzenga *et al.* (2006); 3) Multiple non-linear regression (henceforth named "RF") by Manessa *et al.* (2016a); 4) Second-order polynomial of ratio transform (henceforth named "SPR") by Mishra *et al.* (2006); 5) Principle component (henceforth named "PC") by Van Hengel and Spitzer (1991); four extension of Lyzenga's SDB algorithm by Kanno *et al.* (2011): 6) Multiple linear regression using relaxing uniformity assumption on water and atmosphere (henceforth named "KNW"); 7) Semiparametric regression using depth-independent variables (henceforth named "SMP"); 8) semiparametric regression using spatial coordinates (henceforth named "STR"); 9) Semiparametric regression using depth-independent variables and spatial coordinates (henceforth named "TNP"), and three statistic new statistical approach of Mohamed *et al.* (2017): 10) Bagging Fitting

Ensemble (henceforth named "BAG"); 11) Least Squares Boosting Fitting Ensemble (henceforth named "LSB"); and 12) support vector regression (henceforth named "SVR").

2 MATERIALS AND METHODOLOGY

2.1 Location and Data

2.1.1 Location

This study assesses the performance of twelve empirical models for bathymetry calculations in two different areas: Gili Mantra Islands, West Nusa Tenggara and Menjangan Island, North Bali. First, the Gili Mantra Islands located on the off the coast of Lombok Island. The Gili Mantra Marine Natural Park includes three islands: Gili Trawangan, Gili Meno, and Gili Air (Figure 2-1B). Tourism is the dominant economic activity in the islands. Second, North Bali is the driest area in Bali Islands, due to low rainfall intensity. This condition became a perfect condition for a coral reef to grow. Menjangan Island (Figure 2-1A) is taken as the sample of the site that represent North Bali coral reef area.

2.1.2 Data

2.1.2.1 Single beam sonar

Bathymetry data were measured using a single-beam echo sounder and a differential global positioning system (D-GPS) (plotted as a red dot in Figure 2-1). The bathymetry data of the Gili Islands Island and Menjangan Island is individually collected for research purposed on September 25th, 2011 and September 1st, 2010, respectively. The depth data was strongly affected by tide and wave. Then this study applied a tidal correction (explain further in subchapter 3.1) to reduce the tide effect. But the wave effect is un-corrected and became the drawback issue.

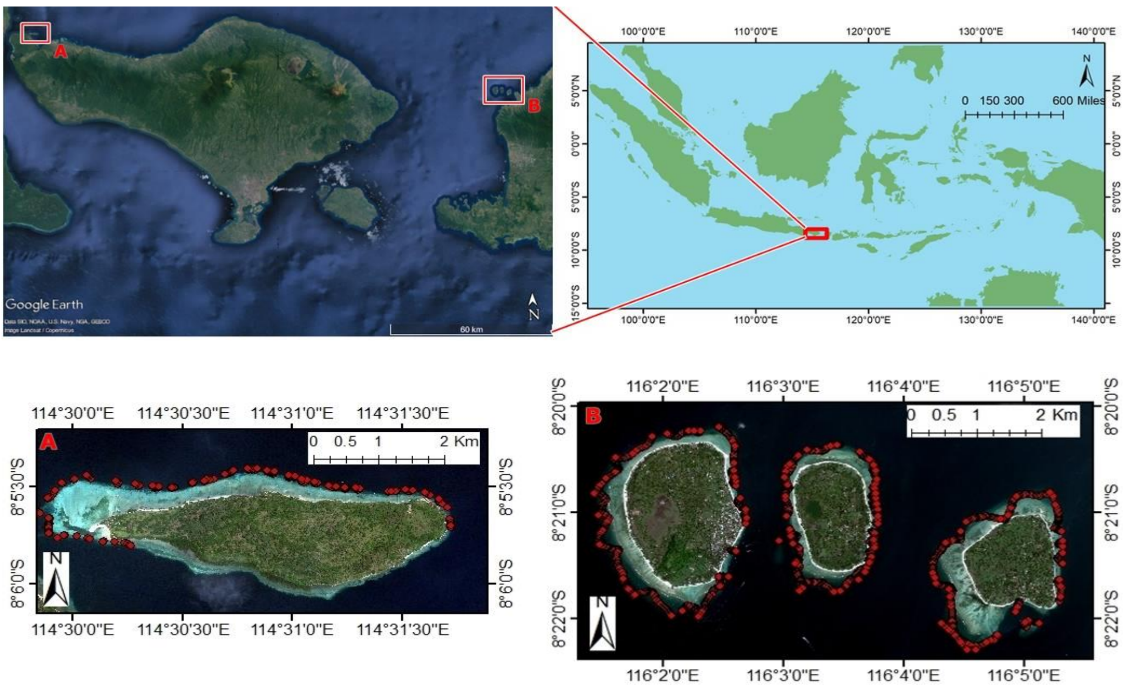

Figure 2-1: Study Site: Indonesia map (upper right), satellite image of Bali island and part of Lombok island (upper left), spot 6 image of Gili Mantra island (under right) and Menjangan island (under left). the red dot shows the depth measurement data

2.1.2.2 Multispectral imagery

The SPOT 6 high-resolution commercial imaging satellite was launched on September 9, 2012. The satellite is in a nearly circular, sun-synchronous orbit with a period of 98.97 minutes at an altitude of approximately 694 km. SPOT 6 acquires 12-bit data in five spectral bands covering blue, green, red, panchromatic, and near-infrared. SPOT 6 image used in this study is shown in Figure 2-1.

2.2 Methods

2.2.1 Tidal Correction

The measured depth data and Multispectral Imagery were affected by the tide. Hence, it necessary to convert the measured depth to zero mean sea levels (MSL) by subtracting the measured depth from the tide level of tide gauge. Also, the Imagery data should tide corrected up to the zero MSL. The tidal data was collected from the Indonesia Geospatial Agency tidal station.

2.2.2 Image Pre-rocessing: Atmospheric and Surface Scattering Correction

The SPOT 6 imagery passed three steps of image pre-processing. The first step was sensor calibration from digital numbers to the units of band-averaged spectral radiance or TOA (Top of Atmosphere) radiance. The equations and calibration coefficients applied were based on the technical note about the radiometric use of SPOT 6 imagery. The physical units of band-averaged spectral radiance are $W \cdot m^{-2} \cdot sr^{-1} \cdot \mu m^{-1}$. Secondly, the atmospheric and surface noise then TOA radiance were corrected (Lyzenga *et al.* 2006). Then, the formula of Lyzenga *et al.* (2006)'s atmospheric dan surface scattering correction is written as:

$$L_{c_i} = L_{TOA_i} - \alpha_{iNIR}.(L_{TOA.NIR} - \bar{L}_{TOA.NIR}) \qquad (2\text{-}1)$$

Where $L_{TOA.NIR1}$ is the measured TOA radiance in NIR band, $\bar{L}_{TOA.NIR}$ is that average over the deep water pixels, and α_{iNIR} is the slope of the simple regression line between the visible radiance and NIR radiance for the deep-water pixels.

Lastly, the relationship between radiance and depth was linearized to create the transformed radiance (X_i). Based on Lyzenga *et al.* (1978), the transformed radiance (X_i) is a linear value of radiance and depth and written as:

$$X_i = log\left(L_{c_i} - \overline{L_c}_{\infty,i}\right) \qquad (2\text{-}2)$$

Where $\overline{L_c}_{\infty,i}$ is the mean of surface radiance deep water area for each band i. The X_i for three visible bands are used as the input for Lyzenga's based model.

2.2.3 Empirical Satellite Derive Bathymetry Algorithm

The twelve empirical algorithm has been choosing intentionally, this algorithm is the most commonly used and also the newest proposed. Several algorithms is a modification of and the first proposed SDB algorithm (Lyzenga 1978; Lyzenga *et al.* 2006). Most of the modification is based on statistical model improvement to nail several unrealistic assumptions, such as the number of bottom types and is based on a premise that bottom radiance is discrete, non-linear relation due to noise influence, and spatial uncorrelatedness of the error term. The summary of SDB empirical algorithm shown in Table 2-1.

2.2.4 Accuracy Assessment

The depth estimation accuracy of each model is measured by (Walpole 1968):

$$R^2 = 1 - \sum_i (h_i - \hat{h}_i)^2 \Big/ \sum_i (h_i - \bar{h})^2 \qquad (2\text{-}3)$$

$$\text{RMSE} = \left(\sum_{i=1}^{n} \left(h_i - \hat{h}_i \right)^2 / n \right)^{0.5} \qquad (2\text{-}4)$$

where h is measurement depth, $\hat{h}$ is estimated depth, $\bar{h}$ is the mean of depth measurement value, and n is the number of input data.

3 RESULTS AND DISCUSSION

Table 3-1 shows the accuracy assessment for the twelve algorithms mention in Table 2-1. In the case of Gili Mantra Island, the RMS errors of the eleven extended methods (PC, LR, LRSPO,

Table 2-1: Summary of 12 models reviewed in this paper

Model	Description and Equation	Source
Principle Component (PC)	Modification algorithm based on Lyzenga's SDB method, based on a rotational transformation of the transformed radiance (X_i), resulting in a depth-dependent variable, i.e. the relative water depth (digital counts), in the direction of the highest variance.	Van Hengel and Spitzer 1991
Linear Ratio (LR)	Proposed to nails the problem of mapping shallow-water areas with significantly lower radiance than adjacent. Accordingly, the change in ratio because of depth is much greater than that caused by a change in bottom albedo, suggesting that different bottom albedoes at a constant depth will still have the same ratio.	Stumpt *et al.* 2003
Second-order Polynomial of Ratio Transform (LRSPO)	Identified a ratio of wavebands (blue and green) that is constant for all bottom types. With these bands having different water absorptions, one band will have arithmetically lesser values than the other. Then, the log ratio of the two bands (blue, green) was plotted against known depth data to develop a second-order polynomial regression.	Mishra *et al.* 2005
Multiple Linear Regression (MLR)	Modified from the simple linear regression (Lyzenga, 1978). In before Lyzenga (1978) used the single band to build the prediction algorithm. The MLR analysis was conducted to depth as the dependent variable and the X_i of all visible bands as the independent variables.	Lyzenga *et al.* 2006
Multiple Linear Regression using Relaxing Uniformity Assumption on Water and Atmosphere (KNW)	Modified the Lyzenga, *et al* 2006, assumed that the water and atmosphere is uniform.	Kanno *et al.* 2011
Semiparametric Regression using Depth-Independent Variables (SMP)	The assumption in Lyzenga *et al.*'s method about the number of bottom types and is based on a premise that bottom radiance is discrete, is unrealistic. Then the elements of the bottom-type-dependent are included and used the semiparametric regression.	Kanno *et al.* 2011
Semiparametric Regression using Spatial Coordinates (STR)	Explicitly model by the spatial dependency of error (ε) due to the assumption of spatial uncorrelatedness of the error term.	Kanno *et al.* 2011
Semiparametric Regression using Depth-Independent Variables and Spatial Coordinates (TNP)	Combined the extension of Relaxing Uniformity Assumption on Water and Atmosphere, Depth-Independent Variables, Spatial Coordinates and uses the semiparametric regression model.	Kanno *et al.* 2011
Multiple Non-Linear Regression (RF)	Theoretically, the relation between depths and linearize surface radiance should be linear but a noise could cause a non-linear condition. Then random forest algorithm is used nail the nonlinear relation between depth and linearized radiance.	Manessa *et al.* 2016a
Bagging Fitting Ensemble (BAG)	The ensemble methods aim at improving the predictive performance of a given statistical learning or model fitting technique. A model is fitted to each bootstrap sample and the models are finally aggregated by majority voting for classification or averaging for regression.	Mohamed *et al.* 2017
Least Squares Boosting Fitting Ensemble (LSB)	The Least Squares Boosting Fitting Ensemble estimation algorithm is built by combining the concept of boosting, ensemble, and least square.	Mohamed *et al.* 2017
Support Vector Regression (SVR)	SVR model is used because of their ability to generalize well with limited training sample that commonly delead with remote sensing. This regression model applied to estimate the depth based on the several pixels with known depth.	Mohamed *et al.* 2017

MLR, KNW, SMP, STR, RF, LSB, BAG, and SVR) were higher compared to TNP method by 1.14, 1.16, 1.15, 0.78, 0.8, 0.65, 0.09, 0.66, 0.99, 0.78, and 0.77m, or in relative terms, 112.9%, 114.9%, 113.9%, 77.2%, 79.2%, 64.4%, 8.9%, 65.3%, 98%, 77.2% and 76.2%, respectively.

In the case of Menjangan Island, the RMS errors of the eleven extended methods (PC, LR, LRSPO, MLR, KNW, SMP, STR, RF, LSB, BAG, and SVR) were also higher compared to TNP method by 0.26, 0.28, 0.28, 0.25, 0.22, 0.18, 0.21, 0.04, 0.24, 0.24, and 0.21 m, or in relative terms, by 23.9%, 25.7%, 25.7%, 22.9%, 20.2%, 16.5%, 19.3%, 3.7%, 22%, 22% and 19.3% respectively. These results indicate that the TNP algorithm effectively improve the accuracy of the other methods.

Based on the results obtained from the image of two evaluated sites, the estimated depth was less accurate in Menjangan Island site. Two processes may have caused these accuracy problems. First, a measurement error of the single beam echo-sounder occurred especially in reef areas with significant morphology different such as Menjangan Island reef, where there were some delays in receiving the signal. Secondly, the significant error of depth measurement due to the data obtained in the afternoon, so high wave occurred. This shows that SDB for coral reef areas has a limitation under a specific condition, proper survey plan (times, instrument, and site) give a significant influence to produce an accurate SDB model.

Scattergrams of the estimated water depth against the measured water depth for Gili Mantra Islands and Menjangan Island are shown in Figure 3-1. The superior accuracy of the TNP algorithm is obvious. Even the other eleven algorithms is based on physical and statistical principles, but still includes several assumptions that are often unrealistic and also not effective or appropriate statistical analysis, details as follows. MLR algorithm assumed that water quality and atmospheric condition is uniform, and the number of bottom types is less than a number of used bands are unrealistic for much shallow water environment

Table 3-1: Statistic value of RMSE and R^2 for depth estimation accuracy of twelve evaluated SDB algorithm (values in bold shows the model with the best accuracy)

Method		Gili Mantra Island		Menjangan Island	
		RMSE [m]	**R^2**	**RMSE [m]**	**R^2**
Van Hengel and Spitzer (1991)	PC	2.15	0.21	1.35	0.16
Stumpt *et al.* (2003)	LR	2.17	0.20	1.37	0.14
Mishra *et al.* (2005)	LRSPO	2.16	0.21	1.37	0.14
Lyzenga *et al.* (2006)	MLR	1.79	0.45	1.34	0.18
Kanno *et al.* (2011)	KNW	1.81	0.44	1.31	0.22
	SMP	1.66	0.53	1.27	0.27
	STR	1.10	0.79	1.30	0.23
	TNP	**1.01**	**0.82**	**1.09**	**0.45**
Manessa *et al.* (2016a)	RF	1.67	0.53	1.13	0.44
Hassan *et al.* (2017)	LSB	2.00	0.32	1.33	0.17
	BAG	1.79	0.44	1.33	0.18
	SVR	1.78	0.48	1.30	0.22

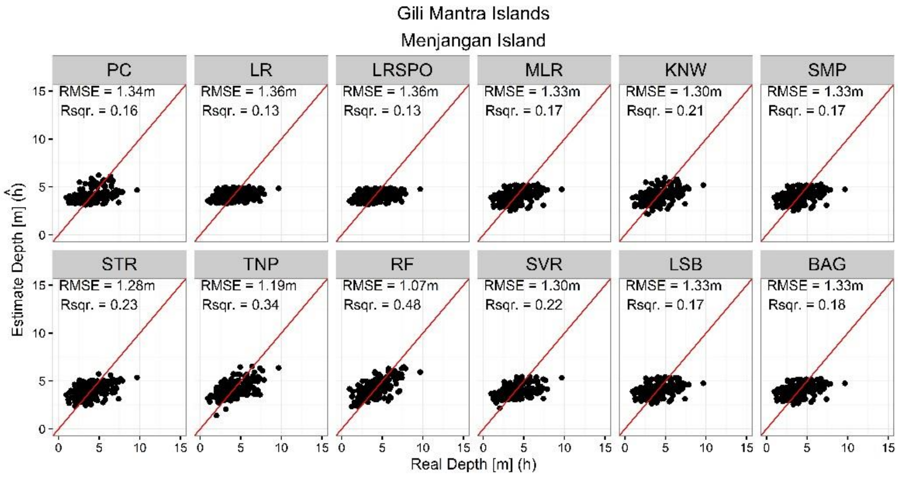

Figure 3-1:Scatter plot between estimated depth and real depth (Rsqr. is equal with R^2) and redlines x=y

(Kanno *et al.* 2011). RF algorithm used in this study is run on auto-tuning mode, however, to get the best result of random forest algorithm, it is necessary to do an optimization on the hyper-parameters (Manessa *et al.* 2016a). LR and PC algorithm focused on noise reduction (Stumpt *et al.* 2003 and Van Hengel and Spitzer 1991) but not consider that the linear regression works well with a number of explanatory variables. The ratio analysis on LR and PC analysis reduces the number of bands (explanatory variables), cause a linear regression of single explanatory variable. LRSPO algorithm used the same assumption with LR algorithm, where a ratio between the blue and green band is plotted with the known depth. Even Mishra *et al.* (2003) in the publication shows that the LRSPO algorithm works well (RMSE = 2,711 m and R^2 = 0.92) but in this study, this algorithm could not produce a good accuracy (RMSE = 1.37 – 2.16 and R^2 = 0.14 – 0.21). KNW algorithm only focuses on non-uniform of surface and atmospheric condition (Kanno *et al.* 2011). SMP algorithm only including the elements of the bottom-type-dependent to nails the premise that bottom radiance is discrete (Kanno *et al.* 2011). STR is proposed only to overcome the assumption of spatial uncorrelatedness of the error term in Lyzenga's method (Kanno *et al.* 2011). Finally, TNP algorithm is a model that nail all the unrealistic assumption mention above (Kanno *et al.* 2011) and also used an advanced statistical analysis (semiparametric regression) to get a satisfactory result. However, it still has a limitation, which requires longer execution times than the other algorithm.

The TNP algorithm used in this study provided a better estimation of depth (Gili Mantra Island RMSE = 1.01 m, Menjangan Island RMSE = 1.09 m) than the other eight algorithms (Gili Mantra Island RMSE = 1.10 - 2.17 m, Menjangan Island RMSE = 1.09 - 1.37 m) under the conditions represented in the study region and images analyzed. This result is in line with the previous studies (Kanno *et al.* 2011, and Arya *et al.* 2017). In the case of the same multispectral image with three visible bands (SPOT-7), the TNP algorithm yielded lower accuracy (RMSE = 1.14 m) (Arya *et al.* 2016) than those reported in this study. The higher RMSE in this study is likely due to differences in environmental conditions, including lower levels of suspended solids of coral reef environment. While for a multispectral image with higher spatial resolution, namely Worldview-2, the TNP algorithm shows higher RMSE value (ranging from 0.2 – 0.8 m) (Kanno *et al.* 2011). This underline just how important the spatial resolution and environment condition on depth estimation accuracy.

4 CONCLUSION

Various empirical models have been developed to convert multispectral image pixel values into depth estimates. This study compares twelve empirical SDB model in two coral reef environment of Indonesia shallow water. In the case of Gili mantra, Islands and Menjangan Island illustrated that depth estimation can be derived from the SPOT 6 multispectral image with accuracy about 1-2 m (RMSE) in water depth down to 15 m. These depth estimation data are useful for many purposes, such as conservation, wave simulation, and coastal zoning. Moreover, as shown in this study, a correct empirical algorithm to be chosen is played an important role to produce an accurate bathymetry map. The accuracy different could reach 3.7 - 114.8% more or less accurate for each empirical algorithm. The result of comparisons suggests that the overall performance of Semiparametric Regression using Depth-Independent Variables and Spatial Coordinates algorithm can produce more accurate depth estimation. This study also found that the effect of wave gave a negative effect on the accuracy of SDB model. Then a wave correction is strongly suggested to be applied to a site with a strong wave influence or exclude an image with that condition.

ACKNOWLEDGEMENTS

The authors extend their appreciation for the support provided by the National Institute of Aeronautics and Space (LAPAN). We would like to thank the Geospatial Information Agency of Indonesia for providing the Gili Mantra Islands and Menjangan Island tidal data. We are very grateful to field survey team and Miko Raharjo. Most importantly, we thank Dr. Ing. Widodo S. Pranowo and Mr. Syarif Budhiman for the scientific advice to improve our manuscript.

REFERENCES

Arya A., Winarso G., Santoso AI, (2016), Ekstraksi Kedalaman Laut Menggunakan Data SPOT 7 di Teluk Belangbelang Mamuju (Accuracy Assesment of Satellite Derived Bathymetry using Lyzenga Method and it's Modification using SPOT 7 Data at the Belangbelang Bay Waters Mamuju). J Ilm Geomatika 22:9–19.

Bierwirth PN, Lee TJ, Burne RV, (1993), Shallow Sea-Floor Reflectance and Water Depth Derived by Unmixing Multispectral Imagery. Photogramm Eng Remote Sensing 59:331–338.

Bramante JF, Raju DK, Sin TM, (2013), Multispectral Derivation of Bathymetry in Singapore's Shallow, Turbid Waters. Int J Remote Sens 34:2070–2088. doi: 10.1080/01431161.2012.734934.

Clark RK, Fay TH, Walker CL, (1987), Bathymetry Calculations with Landsat 4 TM Imagery Under a Generalized Ratio Assumption. Appl Opt 26:4036. doi: 10.1364/AO.26.4036_1.

Conger CL, Hochberg EJ, Fletcher CH, Atkinson MJ, (2006), Decorrelating Remote Sensing Color Bands from Bathymetry in Optically Shallow Waters. IEEE Trans Geosci Remote Sens 44:1655–1660. doi: 10.1109/TGRS. 2006.870405.

Daniell JJ, (2008), Development of a Bathymetric Grid for the Gulf of Papua and Adjacent Areas: A Note Describing its Development. J Geophys Res Earth Surf 113:1–8. doi: 10.1029/2006JF000673.

Deidda M., Sanna G., (2012), Bathymetric Extraction using Worldview-2 High Resolution Images. ISPRS - Int Arch

Photogramm Remote Sens Spat Inf Sci XXXIX-B8:153–157. doi: 10.5194/ isprsarchives-XXXIX-B8-153-2012.

Doxani G., Papadopoulou M., Lafazani P., *et al.,* (2012), Shallow-Water Bathymetry Over Variable Bottom Types Using Multispectral Worldview-2 Image. In: ESA 2nd Space for Hydrology Workshop. 159–164.

Eugenio F., Marcello J., Martin J., (2015), High-Resolution Maps of Bathymetry and Benthic Habitats in Shallow-Water Environments Using Multispectral Remote Sensing Imagery. IEEE Trans Geosci Remote Sens 53:3539–3549. doi: 10.1109/ TGRS.2014.2377300.

Guzinski R., Spondylis E., Michalis M., *et al.,* (2016), Exploring the Utility of Bathymetry Maps Derived With Multispectral Satellite Observations in the Field of Underwater Archaeology. Open Archaeol 2:243–263. doi: 10.1515/opar-2016-0018.

Hernandez W., Armstrong R., (2016), Deriving Bathymetry from Multispectral Remote Sensing Data. J Mar Sci Eng 4:8. doi: 10.3390/jmse4010008.

Hogrefe KR, Wright DJ, Hochberg EJ, (2008), Derivation and Integration of Shallow-Water Bathymetry: Implications for Coastal Terrain Modeling and Subsequent Analyses. Mar Geod 31:299–317. doi: 10.1080/01490410802466710.

Kabiri K., (2017), Accuracy Assessment of Near-Shore Bathymetry Information Retrieved from Landsat-8 Imagery. Earth Sci Informatics 10:235–245. doi: 10.1007/ s12145-017-0293-7.

Kanno A., Koibuchi Y., Isobe M., (2011), Shallow Water Bathymetry from Multispectral Satellite Images: Extensions of Lyzenga'S Method for Improving Accuracy. Coast Eng J 53:431–450. doi: 10.1142/S057856341 1002410.

Kanno A., Tanaka Y., Kurosawa A., Sekine M., (2013), Generalized Lyzenga's Predictor of Shallow Water Depth for Multispectral Satellite Imagery. Mar Geod 36:365–376. doi: 10.1080/01490419.2013.839974.

Kibele J., Shears NT, (2016), Nonparametric Empirical Depth Regression for Bathymetric Mapping in Coastal Waters. IEEE J Sel Top Appl Earth Obs Remote Sens 9:5130–5138. doi: 10.1109/JSTARS.2016. 2598152.

Lafon V., Froidefond J-MM, Lahet F., *et al.*, (2002), SPOT shallow water bathymetry of a moderate turbid tidal inlet based on field measurements. Remote Sens Environ 81:136–148. doi: 10.1016/S0034-4257(01) 00340-6.

Lee K., Kim A., (2011), Determination of bottom-type and bathymetry using WorldView-2. In: Proc. SPIE Ocean Sens. Monitoring III. p 80300D–1.

Liu S., Zhang J., Ma Y., (2010), Bathymetric Ability of SPOT 5 Multi-Spectral Image in Shallow Coastal Water. In: Proc. 18th International Conference on Geoinformatics. 2–6

Lyons M., Phinn S., Roelfsema C., (2011), Integrating Quickbird Multi-Spectral Satellite and Field Data: Mapping Bathymetry, Seagrass Cover, Seagrass Species and Change in Moreton Bay, Australia in 2004 and 2007. Remote Sens 3:42–64. doi: 10.3390/rs3010042.

Lyzenga DR, (1978), Passive Remote Sensing Techniques for Mapping Water Depth and Bottom Features. Appl Opt 17:379. doi: 10.1364/AO.17.000379.

Lyzenga DR, (1985), Shallow-Water Bathymetry Using Combined Lidar and Passive Multispectral Scanner Data. Int J Remote Sens 6:115–125. doi: 10.1080/014311685 08948428.

Lyzenga DR, Malinas NP, Tanis FJ, (2006), Multispectral Bathymetry Using a Simple Physically Based Algorithm. IEEE Trans Geosci Remote Sens 44:2251–2259. doi: 10.1109/TGRS.2006.872909.

Manessa MDM, Kanno A., Sekine M., *et al.,* (2016a), Satellite-Derived Bathymetry Using Random Forest Algorithm and Worldview-2 Imagery. Geoplanning J Geomatics Plan 3:117. doi: 10.14710/geoplanning.3.2.117-126.

Manessa MDM, Kanno A., Sekine M., *et al.*, (2016b), Lyzenga Multispectral Bathymetry Formula for Indonesian Shallow Coral Reef: Evaluation and Proposed Generalized Coefficient. In: Bostater CH, Neyt X, Nichol C, Aldred O (eds) Proc. Remote Sensing of the Ocean, Sea Ice, Coastal Waters, and Large Water Regions 2016. SPIE, Edinburgh, UK, 99990O.

Melsheimer C., Chin LS, (2001), Extracting Bathymetry from Multi-Temporal SPOT Images. In: Proc. The 22nd Asian Conference on Remote Sensing.

Mishra D., Narumalani S., Rundquist D., Lawson M., (2006), Benthic Habitat Mapping in Tropical Marine Environments Using QuickBird Multispectral Data. Photogramm Eng Remote Sensing, 72:1037–1048. doi: 10.14358/PERS.72.9.1037.

Mohamed H., Abdelazim Negm, Salah M., *et al.*, (2017), Assessment of Proposed Approaches for Bathymetry Calculations Using Multispectral Satellite Images in Shallow Coastal/Lake Areas: a Comparison of Five Models. Arab J Geosci 10:1–17. doi: 10. 1007/s12517-016-2803-1.

Pacheco A., Horta J., Loureiro C., Ferreira, (2015), Retrieval of Nearshore Bathymetry From Landsat 8 Images: A Tool for Coastal Monitoring in Shallow Waters. Remote Sens Environ 159:102–116. doi: 10.1016/j.rse. 2014.12.004.

Pushparaj J., Hegde AV, (2017), Estimation of Bathymetry Along the Coast of Mangaluru using Landsat-8 Imagery. Int J Ocean Clim Syst 8:71–83. doi: 10.1177/17593 131166 79672.

Sánchez-Carnero N., Ojeda-Zujar J., Rodríguez-Pérez D., Marquez-Perez J., (2014), Assessment of Different Models for Bathymetry Calculation using SPOT Multispectral Images in a High-Turbidity Area: The Mouth of the Guadiana Estuary. Int J Remote Sens 35:493–514. doi: 10.1080/01431161.2013.871402

Stumpf RP, Holderied K., Sinclair M., (2003), Determination of Water Depth with High-Resolution Satellite Imagery Over Variable Bottom Types. Limnology Oceanogr 48:547–556. doi: 10.4319/lo.2003.48.1_part_2. 0547.

Su H., Liu H., Wang L., *et al.,* (2014), Geographically Adaptive Inversion Model for Improving Bathymetric Retrieval from Satellite Multispectral imagery. IEEE Trans Geosci Remote Sens 52:465–476. doi: 10.1109/TGRS.2013.2241772.

Van Hengel W., Spltzer D., (1991), Multi-Temporal Water Depth Mapping by Means of Landsat TM. Int J Remote Sens 12:703–712. doi: 10.1080/01431169108929687.

Vinayaraj P., Raghavan V., Masumoto S., (2016), Satellite-Derived Bathymetry using Adaptive Geographically Weighted Regression Model. Mar Geod 39:458–478. doi: 10.1080/01490419.2016.1245227.

Walpole RE., (1968), Introduction to Statistics. Macmillan, Madison.

Yuzugullu O., Aksoy A., (2014), Generation of the Bathymetry of a Eutrophic Shallow Lake Using WorldView-2 Imagery. J. Hydroinformatics 16:50. doi: 10.2166/ hydro.2013.133.